Electronic Supplementary Material (ESI) for Catalysis Science & Technology.

ELECTRONIC SUPPLEMENTARY INFORMATION

A simple method to regulate surface hydroxy groups on Al_2O_3 for improving catalytic oxidation performance for HCHO on Pt/Al_2O_3

Zhilin Zhang [a, b], *Jinzhu Ma* [a, b, c]*, *Hong He* [a, b, c]

[a] *State Key Joint Laboratory of Environment Simulation and Pollution Control, Research Center for Eco-Environmental Sciences, Chinese Academy of Sciences, Beijing 100085, China*

[b] *University of Chinese Academy of Sciences, Beijing 100049, China*

[c] *Center for Excellence in Regional Atmospheric Environment and Key Laboratory of Urban Pollutant Conversion, Institute of Urban Environment, Chinese Academy of Sciences, Xiamen 361021, China*

*Corresponding author: Jinzhu Ma jzma@rcees.ac.cn

Experiment Section

Catalyst Characterization. X-ray diffraction (XRD) patterns of the support and catalyst samples were collected with a Bruker D8 X-ray diffractometer with a Cu Kα radiation source (λ = 0.15406 nm). The patterns were measured over the 2θ range from 10° to 90° at a scan step of 0.02°.

The specific surface area and pore characterization of the samples was obtained at -196 °C over the whole range of relative pressures, using a Micromeritics ASAP 2460 analyzer. Prior to the N_2 physisorption, the samples were degassed at 300 °C for 4 h.

Scanning electron microscope (SEM) images were collected on a ZEISS Sigma 500 operated at 3 kV. High resolution transmission electron microscope (HRTEM) images were collected on a JEOL JEM-2100 Plus and JEOL JEM 3200Fs operated at 300 kV.

The actual contents of Pt and Na in catalysts were analyzed using an inductively coupled plasma optical emission spectrometer（ICP-OES）.

High-angle annular dark-field scanning transmission electron microscopy (HAADF-STEM) was performed on a JEOL JEM-ARM 200F with Cs-corrected probe operated at 200 kV.

The in situ diffuse reflectance infrared Fourier transform spectroscopy (DRIFTS) was conducted on an is50 (Thermo Nicolet) FTIR equipped with an MCT/A detector. All spectra were recorded in the range of 4000–800 cm^{-1} by accumulating 90 scans with a resolution of 4 cm^{-1}. A background spectrum was subtracted from each spectrum.

For NH_3-DRIFTS, a background spectrum of N_2 was subtracted from each spectrum. The reduced sample was firstly exposed to a flow of NH_3+N_2 (the concentration of NH_3 was 500 ppm) for 30 min and then purged by N_2 for 30 min.

For CO-DRIFTS, a background spectrum of N_2 was subtracted from each spectrum. The reduced sample was firstly exposed to a flow of CO+N_2 (the concentration of CO was 250 ppm) for 30 min and then purged by N_2 for 30 min.

For HCHO-DRIFTS, a background spectrum of N_2 was subtracted from each spectrum. The reduced sample was exposed to a flow of HCHO+H_2O+N_2 for 30 min.

CO temperature-programmed reduction (CO-TPR), HCHO temperature-programmed desorption (HCHO-TPD) were performed in a Micromeritics AutoChem II 2920 apparatus, equipped with a computer-controlled CryoCooler, a thermal conductivity detector (TCD) and a mass spectrometer detector (MS).

For CO-TPR-MS, the reduced sample was purged by He. After the gas flow was stabilized, the sample temperature was increased from 30 ^{o}C to 500 ^{o}C at a ramping rate of 10 ^{o}C min^{-1}. The CO_2 and H_2 production were monitored by the mass spectrometer detector at a m/z ratio of 44 and 2, respectively.

For HCHO-TPD-MS, the reduced sample was firstly exposed to a flow containing 20% O_2, 35 % water vapor and 110 ppm HCHO for 1 h at room temperature in the fixed-bed quartz flow reactor. After that, the sample was transformed to the sample warehouse of Micromeritics AutoChem II 2920 instrument and the temperature was cooled down to 25 ^{o}C in He gas flow. The sample was subjected to a He purge for 30 min, then HCHO-TPD was conducted in He gas flow from 25 ^{o}C to 500 ^{o}C at a ramping rate of 10 ^{o}C min^{-1}. The desorbed H_2, CO, HCHO and CO_2 were monitored using the mass spectrometer at m/z ratios of 2, 28, 30 and 44, respectively.

The inlet and outlet gases detector. The inlet and outlet gases were monitored by FTIR (Nicolet 380) equipped with 2 m gas cell and a DTGS detector; resolution: 0.5 cm^{-1}; OPD velocity: 0.4747 cm s^{-1}. The collection region was 4000-400 cm^{-1} and the number of scans per spectrum was 32. HCHO and CO_2 were measured by the peaks located at 2897 (C-H vibration) and 2350 cm^{-1} (O-C-O vibration), respectively. Since no other carbon-containing compounds except for CO_2 were detected in the effluents for all tested catalysts, the HCHO and CO_2 concentrations were quantified and calculated based on the peak area of CO_2 at 2350 cm^{-1}. Before the measurement, a CO_2 standard curve was created using the different CO_2 concentrations versus the peak areas at 2350 cm^{-1}.

Table S1. The specific surface area (S_{BET}) of the supports and catalysts.

Sample	S_{BET} (m^2/g)	Sample	S_{BET} (m^2/g)
Al-2h	358	Pt-Na/Al-2h	339
Al-3h	369	Pt-Na/Al-3h	341
Al-4h	365	Pt-Na/Al-4h	349
Al-5h	369	Pt-Na/Al-5h	348

Table S2. Pt content and Na content of Pt-Na/Al-2h, Pt-Na/Al-3h, Pt-Na/Al-4h and Pt-Na/Al-5h.

Sample	Pt content (%)	Na content (%)
Pt-Na/Al-2h	0.05	0.85
Pt-Na/Al-3h	0.05	0.84
Pt-Na/Al-4h	0.05	0.86
Pt-Na/Al-5h	0.05	0.86

Table S3. NH_3-DRIFTS results of Al-x supports and Pt-Na/Al-x catalysts.

Sample	Wavenumbers and Related Content (%)			
	3761 cm^{-1} HO-μ_{ter}	3752 cm^{-1} HO-$\mu_{bri(Na-Al)}$	3736 cm^{-1} HO-$\mu_{bri(Al-Al)}$	3677 cm^{-1} HO-μ_{tri}
Al-5h	27.7	-	49.7	22.6
Al-4h	29.1	-	50.3	20.6
Al-3h	19.8	-	57.1	23.2
Al-2h	-	-	65.1	34.9
Pt-Na/Al-5h	-	70.2	13.5	16.3
Pt-Na/Al-4h	-	64.6	19.2	16.2
Pt-Na/Al-3h	-	46.4	30.1	23.5
Pt-Na/Al-2h	-	42.5	29.3	28.2

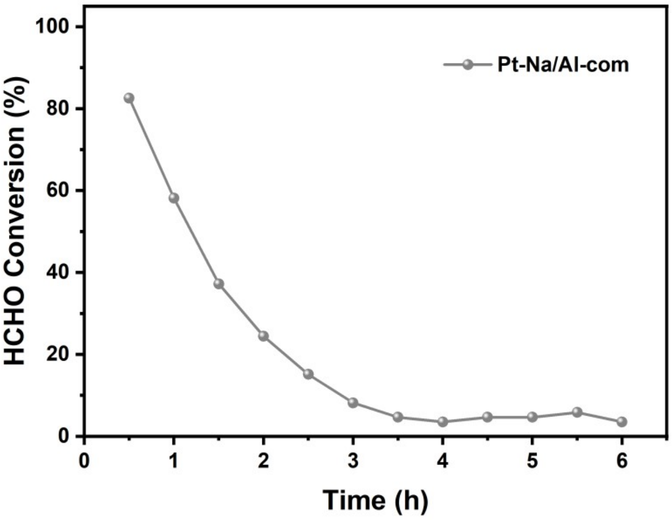

Figure S1. HCHO catalytic oxidation performance of Pt-Na/Al-com. Reaction conditions: 25 °C, 110 ppm of HCHO, 20 vol % O_2, 35 % RH, N_2 balanced and WHSV of 200 000 mL/ (g h).

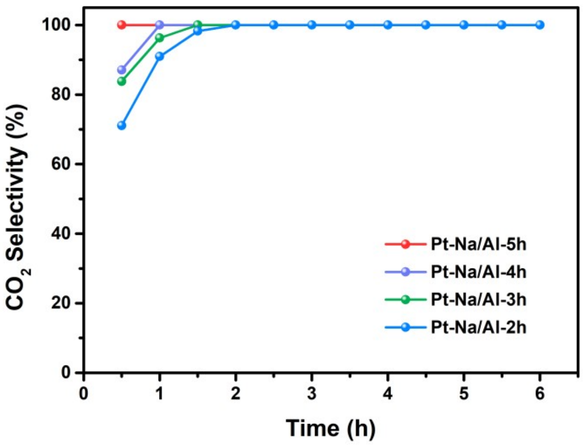

Figure S2. CO_2 selectivity of Pt-Na/Al-2h, Pt-Na/Al-3h, Pt-Na/Al-4h and Pt-Na/Al-5h. Reaction conditions: 25 ^{o}C, 110 ppm of HCHO, 20 vol % O_2, 35 % RH, N_2 balanced and WHSV of 200 000 mL/ (g h).

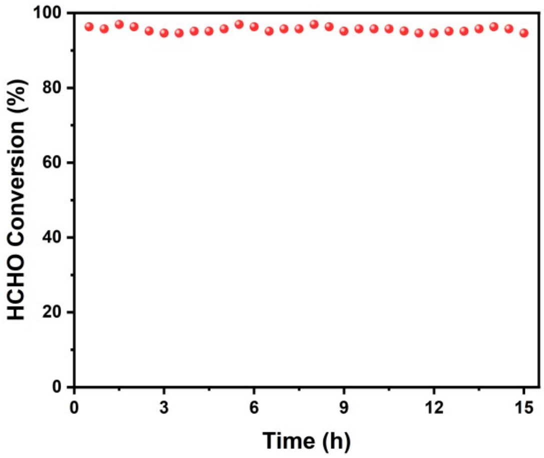

Figure S3. The HCHO oxidation stability of Pt-Na/Al-5h. Reaction conditions: 25 ^{o}C, 180 ppm of HCHO, 20 vol % O_2, 35 % RH, N_2 balanced and WHSV of 120 000 mL/(g h).

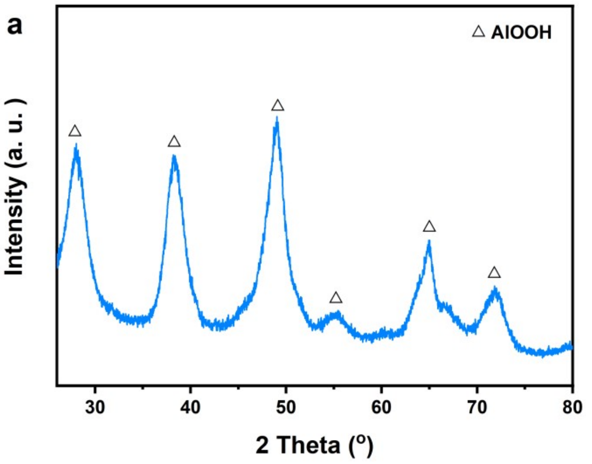

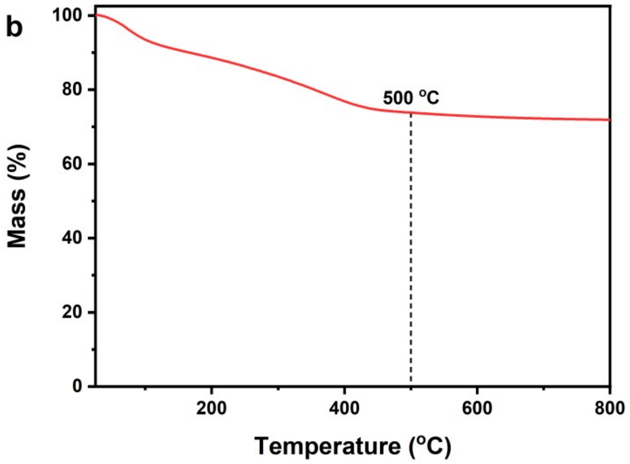

Figure S4. The a) XRD pattern and b) TG curve of AlOOH.

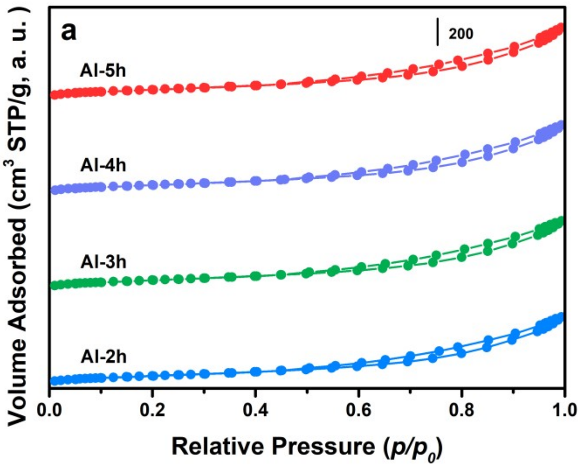
a
200
Al-5h
Al-4h
Al-3h
Al-2h
0.0
0.2
0.4
0.6
0.8
1.0
Relative Pressure (p/p_0)
Volume Adsorbed (cm^3 STP/g, a. u.)

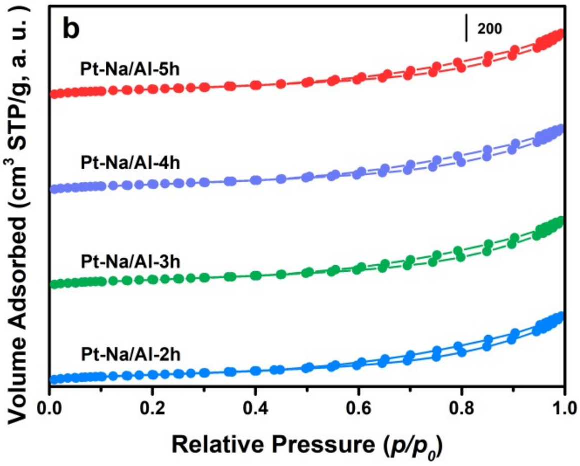
b
200
Pt-Na/Al-5h
Pt-Na/Al-4h
Pt-Na/Al-3h
Pt-Na/Al-2h
0.0
0.2
0.4
0.6
0.8
1.0
Relative Pressure (p/p_0)
Volume Adsorbed (cm^3 STP/g, a. u.)

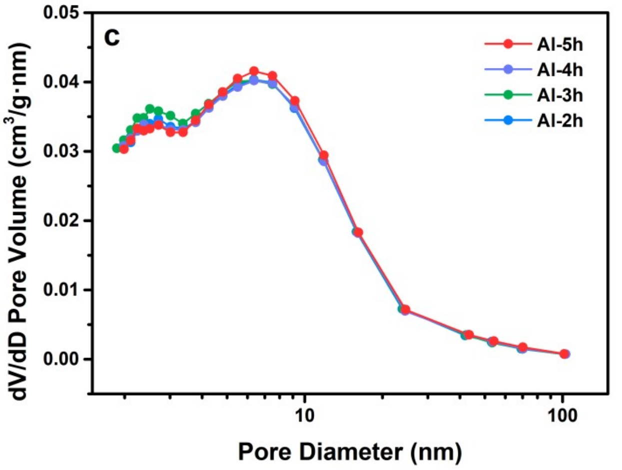
c
Al-5h
Al-4h
Al-3h
Al-2h
0.05
0.04
0.03
0.02
0.01
0.00
10
100
Pore Diameter (nm)
dV/dD Pore Volume (cm^3/g·nm)

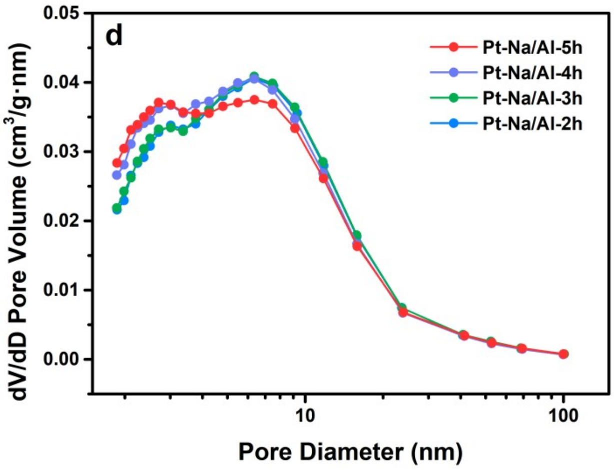

Figure S5. N_2 adsorption-desorption isotherms and the corresponding pore size distributions of Al-2h, Al-3h, Al-4h and Al-5h supports, and Pt-Na/Al-2h, Pt-Na/Al-3h, Pt-Na/Al-4h and Pt-Na/Al-5h catalysts.

Figure S6. HRTEM images of a) AlOOH, b) Al-2h and c) Al-5h supports.

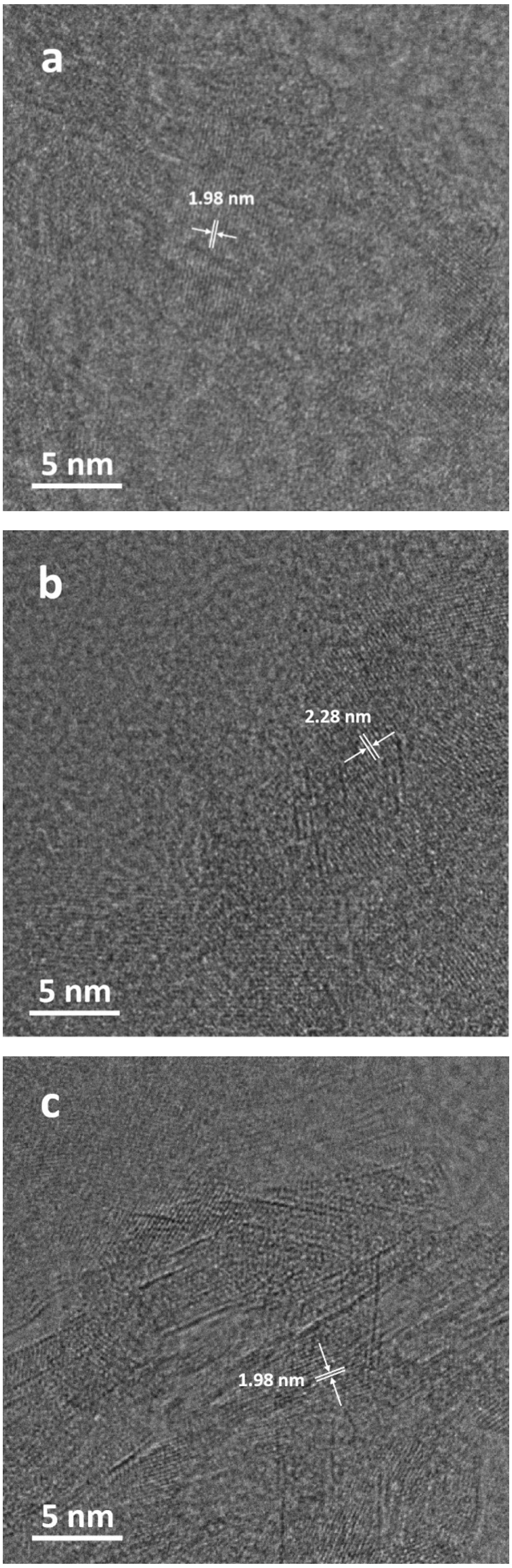

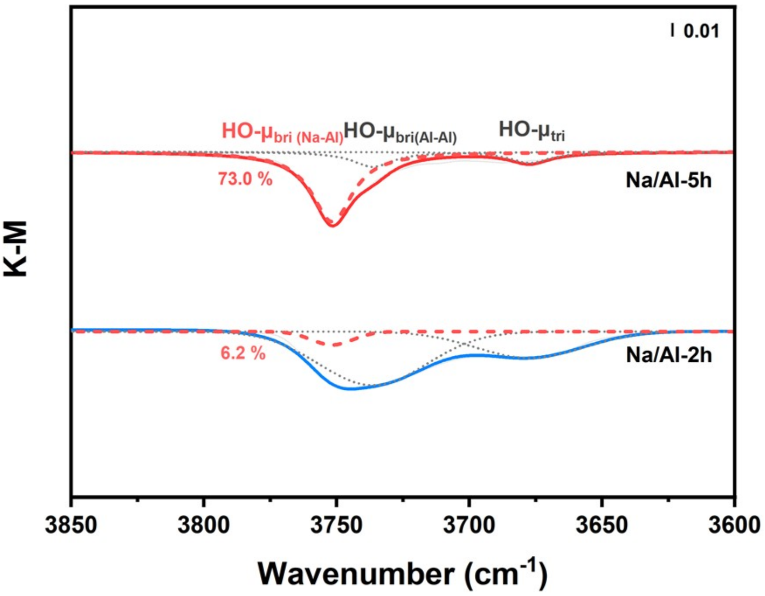

Figure S7. In-situ DRIFTS results of NH_3 adsorption of Na/Al-x samples.

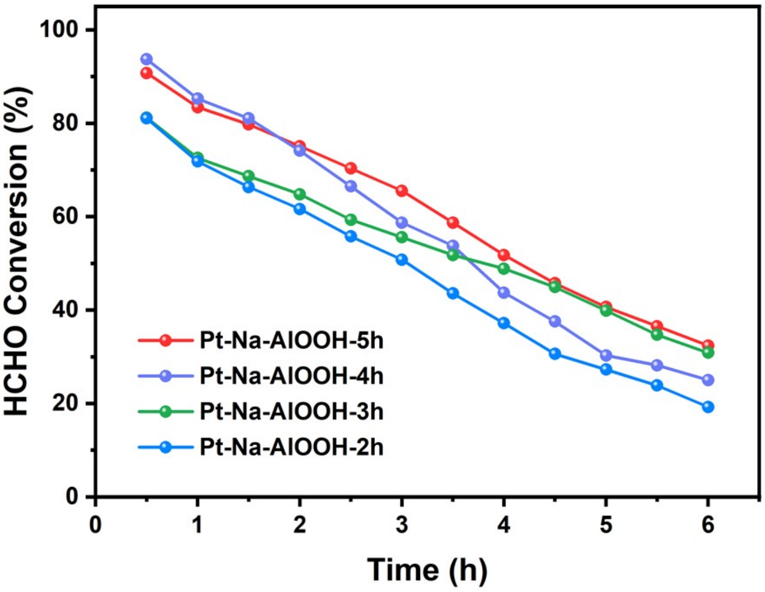

Figure S8. HCHO catalytic oxidation performance of Pt-Na-AlOOH-2h, Pt-Na-AlOOH-3h, Pt-Na-AlOOH-4h and Pt-Na-AlOOH-5h. Reaction conditions: 25 ^{o}C, 110 ppm of HCHO, 20 vol % O_2, 35 % RH, N_2 balanced and WHSV of 200 000 mL/ (g h).

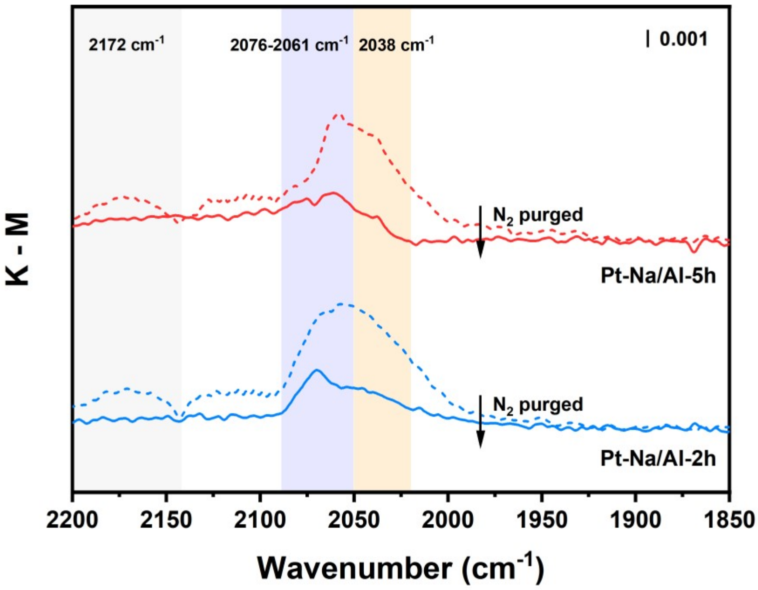

Figure S9. In-situ DRIFTS results of Pt-Na/Al-2h and Pt-Na/Al-5h at 30 °C. Reaction condition: CO+N_2 adsorption for 30 min, N_2 purged for 30 min.

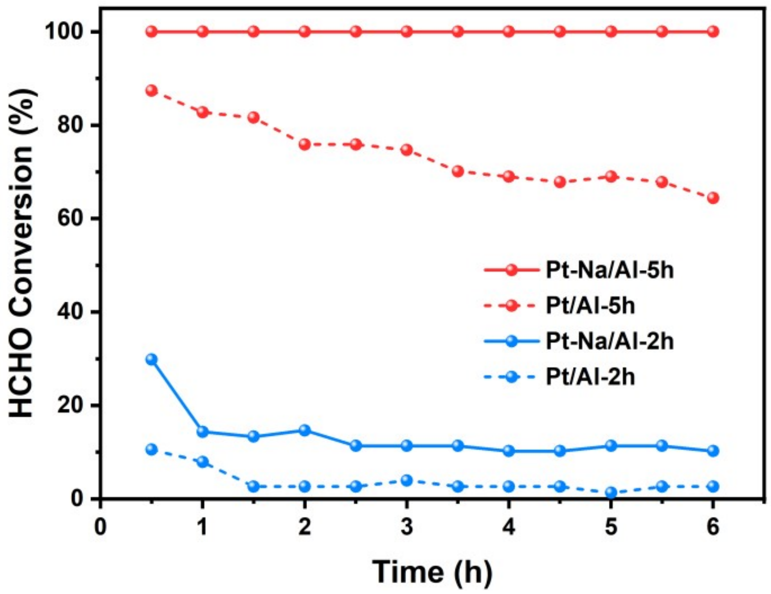

Figure S10. HCHO catalytic oxidation performance of Pt-Na/Al-5h, Pt-Na/Al-2h, Pt/Al-5h and Pt/Al-2h. Reaction conditions: 25 ℃, 110 ppm of HCHO, 20 vol % O_2, 35 % RH, N_2 balanced and WHSV of 200 000 mL/ (g h).

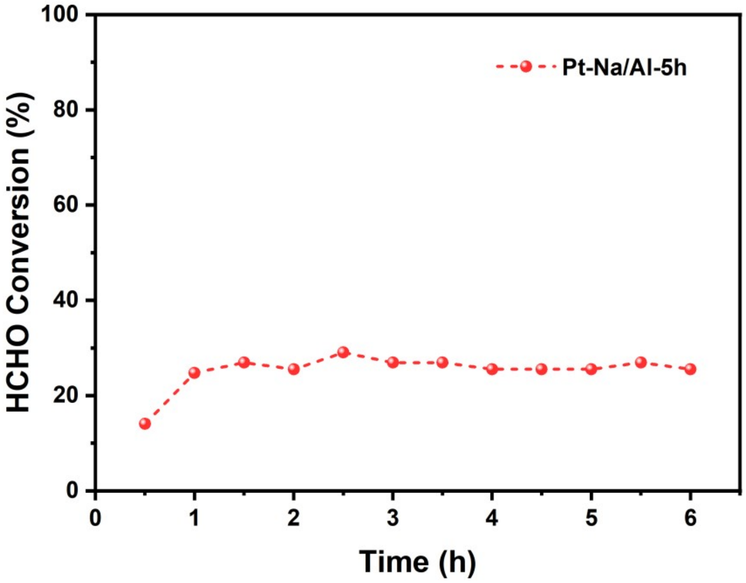

Figure S11. HCHO catalytic oxidation performance of Pt-Na/Al-5h. Reaction conditions: 25 ℃, 110 ppm of HCHO, 20 vol % O_2, 0 % RH, N_2 balanced and WHSV of 200 000 mL/ (g h).